

Recent Results from BESIII

Guangshun Huang (Representing the BESIII Collaboration)

Department of Modern Physics, University of Science and Technology of China,
96 JinZhai Road, Hefei, Anhui, 230026, P.R.China

BESIII is a new state-of-the-art 4π detector at the upgraded BEPCII two-ring e^+e^- collider at the Institute of High Energy Physics in Beijing, China. It has been in operation since 2008, and has collected the world's largest data samples of J/ψ , ψ' and $\psi(3770)$ decays, as well as τ mass scan and low energy points for R measurement. These data are being used to make a variety of interesting and unique studies of light-hadron spectroscopy, precision charmonium physics, high-statistics measurements of D meson decays, τ mass measurement and R measurement. Results summarized in this report include observations of a subthreshold $p\bar{p}$ resonance in $J/\psi \rightarrow \gamma p\bar{p}$, a large isospin-violation in $\eta(1405) \rightarrow \pi^0 f_0(980)$ decays, a near-threshold enhancement in $J/\psi \rightarrow \gamma \omega \phi$, and a M1 transition $\psi' \rightarrow \gamma \eta_c(2S)$; the $\rho\pi$ puzzle in J/ψ and ψ' decays; some recent precision measurements of η_c and h_c lineshapes; and preliminary results of the D meson (semi-)leptonic decays and the τ mass measurement.

I. INTRODUCTION

The BES experimental program dates back to late 1989 when operation of the Beijing Electron Positron Collider (BEPC) and the Beijing Electron Spectrometer (BES) first started. BEPC was a single-ring e^+e^- collider that operated in the τ -charm threshold energy region between 2.0 and 5.0 GeV with a luminosity of $\sim 10^{31} \text{cm}^{-2}\text{s}^{-1}$. Among the early successes included a precise measurement of the mass of the τ lepton [1] that not only improved on the precision of previous measurements by an order-of-magnitude, but also showed that the existing world average value was high by about two standard deviations. In the late 1990s, the BES detector was upgraded to the BESII detector and this produced another key result that was the precise measurement of the total cross section for e^+e^- annihilation into hadrons (R value) over the accessible center of mass (c.m.) energy range [2, 3]. The precision of these measurements lead to a substantially improved evaluation of the electromagnetic coupling constant extrapolated to the Z -boson mass peak, $\alpha_{QED}(M_Z^2)$, which resulted in a significant $\sim 30\%$ increase in the Standard Model (SM) predicted value for the Higgs' boson mass [4]. BESII also discovered a number of new hadron states, including the σ [5] and κ [6] scalar resonances and a still-unexplained subthreshold $p\bar{p}$ resonance produced in radiative $J/\psi \rightarrow \gamma p\bar{p}$ decays [7].

Between 2005 and 2008, BEPC was replaced by BEPCII, a two-ring e^+e^- collider with a hundred-fold increase in luminosity, and the BESII detector was completely removed and replaced by BESIII, a state-of-the-art detector built around a 1 T superconducting solenoid that contains a cylindrical drift chamber, a double-layer barrel of scintillation counters for time-of-flight measurements, and a nearly 4π array of 6240 CsI(Tl) crystals for electromagnetic calorimetry. The magnet's iron flux-return yoke is instrumented with a nine-layer RPC muon identification system. BEPCII operations started in summer 2008 and since then the luminosity has been continuously improving; now it is $\sim 6.5 \times 10^{32} \text{cm}^{-2}\text{s}^{-1}$, quite near the 10^{33} design value. The BESIII detector performance is excellent: the charged particle momentum resolution is $\delta p/p \simeq 0.5\%$; the γ energy resolution is 2.5% at $E_\gamma = 1$ GeV; the 6% resolution dE/dx measurements in the drift chamber plus the ~ 80 ps resolution time-of-flight measurements is sufficient to identify charged particles over the entire momentum range of interest.

The BESIII experimental program addresses issues in light hadron physics, charmonium spectroscopy and decays, D and D_s meson decays, and numerous topics in QCD and τ -lepton physics. To date, BESIII has accumulated data samples corresponding to 225M (plus $\sim 1.0\text{B}$ in 2012) J/ψ decays, 106M ($+$ $\sim 0.4\text{B}$) ψ' decays, 2.9fb^{-1} at the peak of the $\psi(3770)$ resonance, which decays to $D\bar{D}$ meson pairs nearly 100% of the time, 24pb^{-1} around τ -pair threshold, and $10k$ hadronic events at each of 4 low energies. These are all world's-largest data samples at these c.m. energies and the J/ψ sample is the first ever to be collected in a high quality detector like BESIII. In this talk I review some

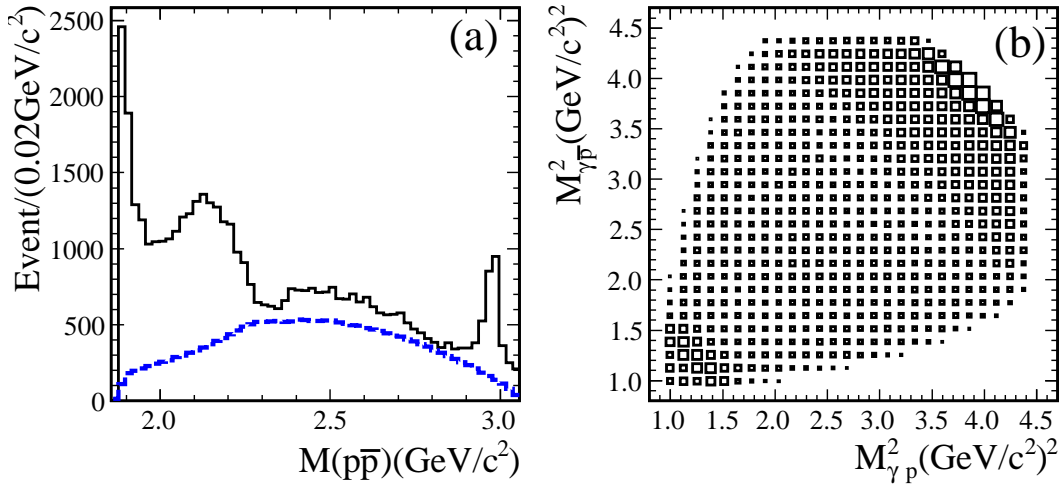


FIG. 1: **a)** The $M(p\bar{p})$ distribution from $J/\psi \rightarrow \gamma p\bar{p}$ decays. The dashed curve is background from $J/\psi \rightarrow \pi^0 p\bar{p}$, where one of the photons from the $\pi^0 \rightarrow \gamma\gamma$ decay has low energy and is undetected. The narrow peak on the right is from $J/\psi \rightarrow \gamma\eta_c$, $\eta_c \rightarrow p\bar{p}$. **b)** The $M^2(\gamma\bar{p})$ (vertical) vs. $M^2(\gamma p)$ Dalitz plot for the same data sample. The diagonal band at the upper right is produced by the $p\bar{p}$ mass-threshold enhancement; the band at the lower left is due to the η_c .

recent results that have been generated from these data samples.

II. LIGHT HADRON PHYSICS

A. The subthreshold $p\bar{p}$ resonance seen in $J/\psi \rightarrow \gamma p\bar{p}$

As mentioned above in the introduction, BESII reported a peculiar mass-threshold enhancement in the $p\bar{p}$ invariant mass distribution in radiative $J/\psi \rightarrow \gamma p\bar{p}$ decays [7]. The shape of this low-mass peak cannot be reproduced by any of the commonly used parameterizations for final state interactions (FSI) between the final-state p and \bar{p} .

The $p\bar{p}$ invariant mass distribution for $J/\psi \rightarrow \gamma p\bar{p}$ decays in the 225M event BESIII J/ψ data sample is shown in Fig. 1a, where the threshold enhancement is quite prominent [8]. A Dalitz plot for these events is shown in Fig. 1b. A partial-wave-analysis (PWA) applied to these data determined that the J^{PC} of the near-threshold structure is 0^{-+} . A fit using a sub-threshold resonance shape modified by the Julich FSI effects [9] yields a mass of $M = 1832^{+32}_{-26}$ MeV and a 90% CL upper limit on the width of $\Gamma < 79$ MeV.

B. Isospin violations in $\eta(1405)$ decays

BESIII examined the $\pi^0 f_0$ invariant mass distribution produced in radiative $J/\psi \rightarrow \gamma\pi^0 f_0$ decays for both the $f_0 \rightarrow \pi^+\pi^-$ and $f_0 \rightarrow \pi^0\pi^0$ decay modes [10]. In the distribution for $f_0 \rightarrow \pi^0\pi^0$ decays, shown in the left panel of Fig. 2 (the $f_0 \rightarrow \pi^+\pi^-$ channel looks similar), the dominant feature is a pronounced peak near $M(\pi^0 f_0) = 1405$ MeV; helicity analyses indicate that this peak has $J^P = 0^-$, which leads to its identification as the $\eta(1405)$ resonance.

The decay $\eta(1405) \rightarrow \pi^0 f_0$ violates isospin. In this case the observed isospin violation is quite large:

$$\frac{Bf(\eta(1405) \rightarrow \pi^0 f_0(980) \rightarrow \pi^0 \pi^+ \pi^-)}{Bf(\eta(1405) \rightarrow \pi^0 a_0(980) \rightarrow \pi^0 \pi^0 \eta)} = (17.9 \pm 4.2)\%, \quad (1)$$

which is an order-of-magnitude larger than is typical for isospin violations. (For example, BESIII also reports that the isospin violating $Bf(\eta' \rightarrow \pi^+\pi^-\pi^0)$ is $(0.9 \pm 0.1)\%$ of the isospin conserving $Bf(\eta' \rightarrow \pi^+\pi^-\eta)$ [10].)

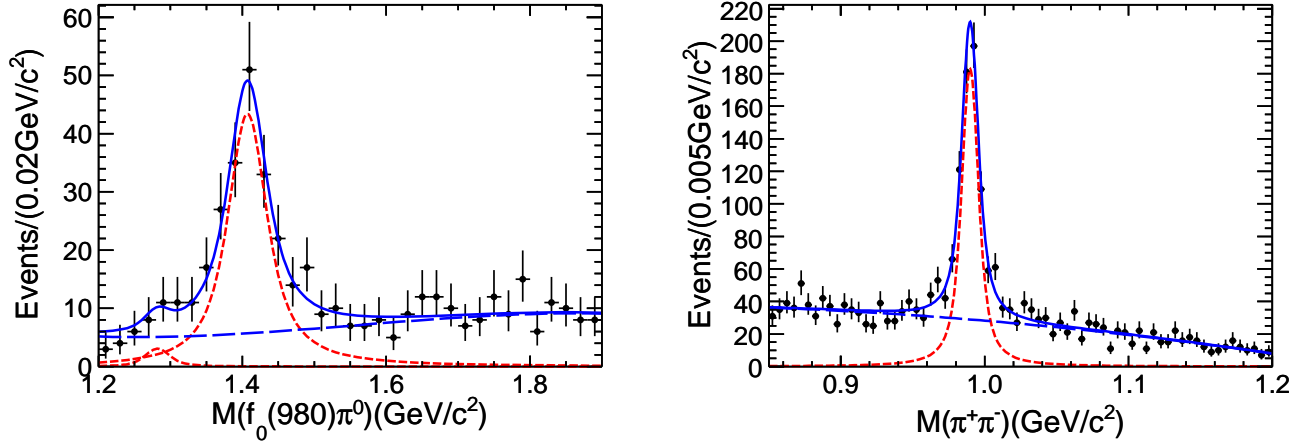


FIG. 2: **Left:** The $\pi^0 f_0$ mass distribution from $J/\psi \rightarrow \gamma \pi^0 f_0$, decays where $f_0 \rightarrow \pi^0 \pi^0$ (a $J/\psi \rightarrow 7\gamma$ final state!). **Right:** The $\pi^+\pi^-$ mass distribution from $\eta(1405) \rightarrow \pi^0 f_0$ decays where $f_0 \rightarrow \pi^+\pi^-$.

A striking feature of these decays is the lineshape of the $f_0 \rightarrow \pi\pi$ decays, shown for the $f_0 \rightarrow \pi^+\pi^-$ channel in the right panel of Fig. 2, where it can be seen that the f_0 peak position is significantly above its nominal 980 MeV value, and its width is much narrower than its nominal value of ~ 100 MeV. The fitted mass is $M = 989.9 \pm 0.4$ MeV, midway between $2m_{K^+}$ and $2m_{K^0}$, and the fitted width is $\Gamma = 9.5 \pm 1.1$ MeV, consistent with the $2m_{K^0} - 2m_{K^+} = 7.8$ MeV mass threshold difference.

Possible processes that mediate $\eta(1405) \rightarrow \pi^0 f_0$ are shown in Fig. 3. As we have seen above, the $a_0(980) \rightarrow f_0(980)$ process (Fig. 3a) is at or below the percent level, and is too small to account for the large isospin violation that is observed. Wu and collaborators [11] suggest that the triangle anomaly diagram shown in Fig. 3b could be large enough to account for the data. In this case, both the $K^*\bar{K}$ system that couples to the $\eta(1405)$ and the $K\bar{K}$ system coupling to the f_0 can have large on-mass-shell, isospin-violating contributions.

While our understanding of the low mass scalar mesons remains unclear, it seems that detailed studies – both theoretical and experimental – of isospin violations in processes involving the $a_0(980)$ and $f_0(980)$ can provide important probes of their inner workings. The results presented above are from data samples that are small fractions of what we ultimately expect to collect with BESIII. With the full data sets we will be able to provide theorists with precision measurements of the $a_0(980) \leftrightarrow f_0(980)$ mixing parameters and other quantities related to these mesons.

C. $J/\psi, \psi' \rightarrow 3\pi$ and the $\rho\pi$ puzzle

The oldest puzzle in charmonium physics is the so-called $\rho\pi$ puzzle. $J/\psi \rightarrow \rho\pi$ is the strongest hadronic decay mode of the J/ψ , with a branching fraction of $(1.69 \pm 0.15)\%$ [12]. The lowest-order diagram for this decay is expected to be the three-gluon annihilation process. The same diagram is expected to apply to the ψ' and, thus, the partial width $\Gamma(\psi' \rightarrow \rho\pi)$ is expected to be that for the J/ψ , scaled by the ratio of the $c\bar{c}$ wavefunctions at the origin and a phase-space factor. (The ratio of the wavefunctions at the origin is determined by comparing the $J/\psi \rightarrow e^+e^-$ and $\psi' \rightarrow e^+e^-$ partial widths.) The result of this reasoning is the famous “12% rule,” which says that the branching fraction for ψ' to some hadronic state should be (roughly) 12% that of the J/ψ to the same final state. While this simple rule more-or-less works for many decay modes, it fails miserably for $\psi' \rightarrow \rho\pi$ decays, where $Bf(\psi' \rightarrow \rho\pi) = (3.2 \pm 1.2) \times 10^{-5}$, nearly a factor of a hundred below the 12%-rule expectation.

BESIII has recently reported on a high-statistics study of $J/\psi \rightarrow \pi^+\pi^-\pi^0$ and $\psi' \rightarrow \pi^+\pi^-\pi^0$ [13] using the 225M event J/ψ and 106M event ψ' data samples. The $M^2(\pi^-\pi^0)$ (vertical) *vs.* $M^2(\pi^+\pi^0)$ (horizontal) Dalitz plot distributions, shown in the top panels of Fig. 4, for the J/ψ (left) and ψ' (right) data samples, could not be more different. The center of the $J/\psi \rightarrow \pi^+\pi^-\pi^0$ Dalitz plot is completely devoid of events, while in the $\psi' \rightarrow \pi^+\pi^-\pi^0$

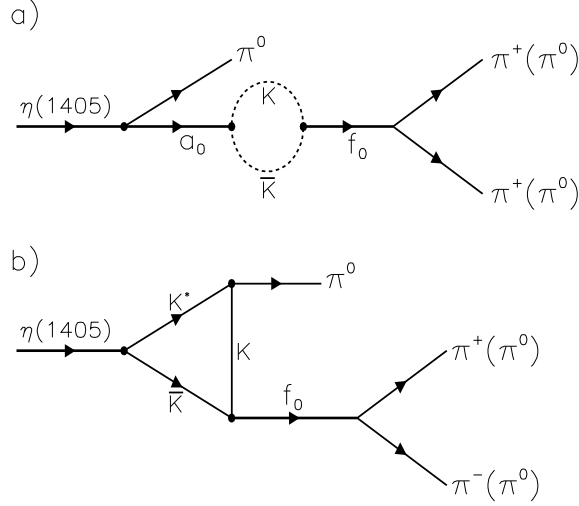


FIG. 3: **a)** The leading diagram for $\eta(1405) \rightarrow \pi^0 f_0$ via $a_0(980)$ - $f_0(980)$ mixing. **b)** The triangle anomaly diagram in $\eta(1405) \rightarrow \pi^0 f_0(980)$ decay [11].

plot most of the events are concentrated in the center. The dynamics of the two processes are completely different, in spite of the fact that the underlying process is expected to be very similar. The $\rho\pi$ puzzle is becoming even more puzzling.

D. Near-threshold enhancement in $J/\psi \rightarrow \gamma\omega\phi$

An anomalous enhancement near threshold in the invariant-mass spectrum of $\omega\phi$, denoted as $X(1810)$, was first reported by the BESII experiment in the decays of $J/\psi \rightarrow \gamma\omega\phi$ with a statistical significance of larger than 10σ [14]. A partial wave analysis (PWA) of BESII data with a helicity covariant amplitude showed that the $X(1810)$, with a mass and width of $M = 1812_{-26}^{+19} \pm 18$ MeV/ c^2 , and $\Gamma = 105 \pm 20 \pm 28$ MeV/ c^2 , respectively, and a product branching fraction $\mathcal{B}(J/\psi \rightarrow \gamma X(1810)) \cdot \mathcal{B}(X(1810) \rightarrow \omega\phi) = [2.61 \pm 0.27 \pm 0.65] \times 10^{-4}$, favors $J^{PC} = 0^{++}$ over $J^{PC} = 0^{-+}$ or 2^{++} . The decay of $J/\psi \rightarrow \gamma\omega\phi$ is a doubly OZI suppressed process with a production rate that is suppressed relative to $J/\psi \rightarrow \gamma\omega\omega$ or $J/\psi \rightarrow \gamma\phi\phi$ by at least one-order-of-magnitude [15]. The observation of $X(1810)$ has stimulated much theoretical speculation. Possible interpretations of $X(1810)$ include a tetraquark state (with structure $q^2\bar{q}^2$) [16], a hybrid [17], a glueball state [18], an effect due to the intermediate meson rescattering [19], a threshold cusp attracting a resonance [20], etc. As of now, none of these interpretations has either been established or ruled out by experiment. A search for the $X(1810)$ was performed by the Belle collaboration in the decay of $B^\pm \rightarrow K^\pm\omega\phi$ [21], but no obvious $X(1810)$ signal was observed.

Using 2.25×10^8 J/ψ events, BESIII has re-studied the decay of $J/\psi \rightarrow \gamma\omega\phi$, $\omega \rightarrow \pi^+\pi^-\pi^0$, $\phi \rightarrow K^+K^-$. The enhancement structure near the $\omega\phi$ invariant-mass threshold is confirmed with a statistical significance larger than 30σ . A partial wave analysis with a tensor covariant amplitude confirms that the spin-parity of $X(1810)$ is 0^{++} . The mass and width of the $X(1810)$ are determined to be $M = 1795 \pm 7_{-5}^{+23}$ MeV/ c^2 and $\Gamma = 95 \pm 10_{-34}^{+78}$ MeV/ c^2 , respectively, and the product branching fraction is $\mathcal{B}(J/\psi \rightarrow \gamma X(1810)) \times \mathcal{B}(X(1810) \rightarrow \omega\phi) = (2.00 \pm 0.08_{-1.00}^{+1.38}) \times 10^{-4}$, where the first error is statistical and the second systematical. These preliminary results are consistent with

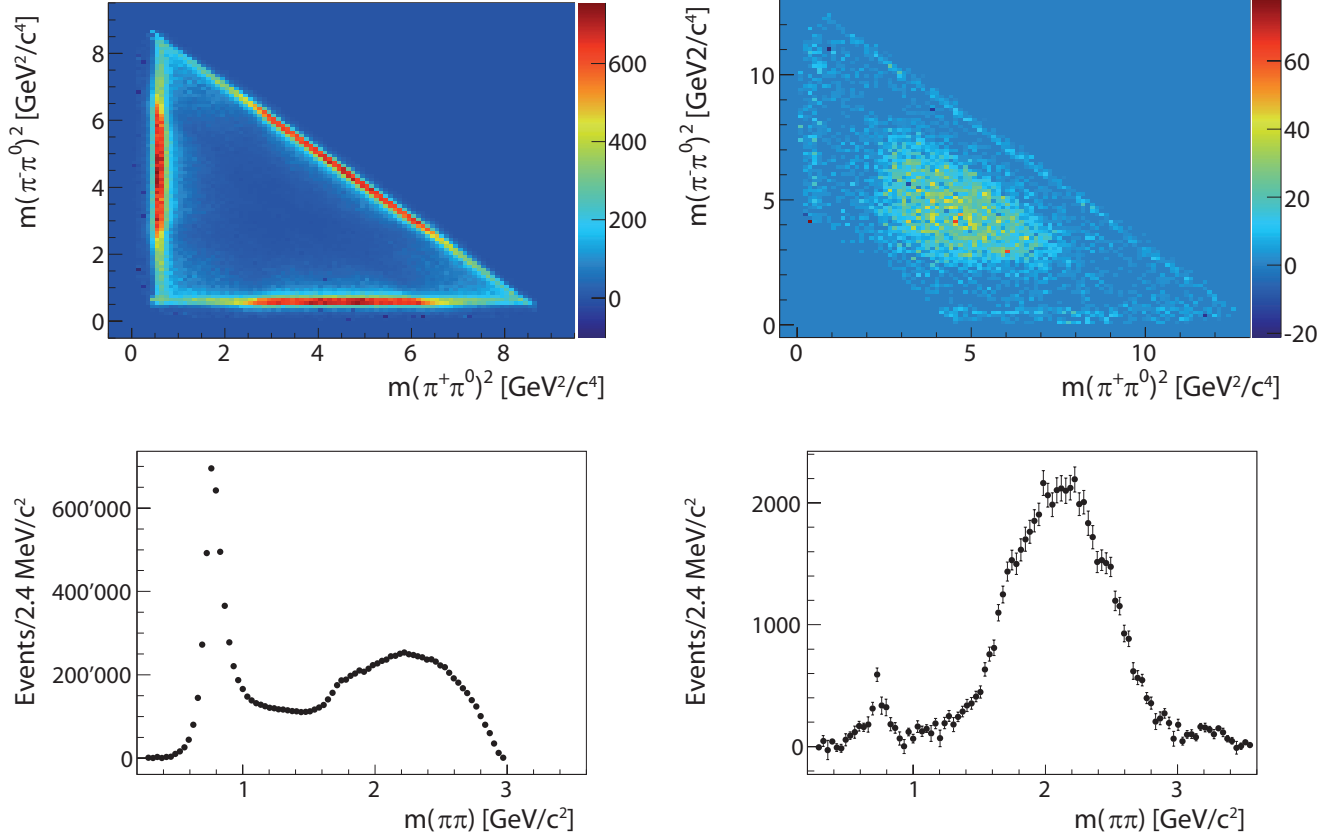


FIG. 4: **Top:** the $M^2(\pi^-\pi^0)$ (vertical) vs. $M^2(\pi^+\pi^0)$ (horizontal) for (left) $J/\psi \rightarrow \pi^+\pi^-\pi^0$ and (right) $\psi' \rightarrow \pi^+\pi^-\pi^0$ decays. **Bottom:** the $M(\pi\pi)$ projections of the Dalitz plots.

those from BESII within errors. Fig. 5 shows the invariant mass spectrum of $K^+K^-\pi^+\pi^-\pi^0$ and the Dalitz plot.

III. CHARMONIUM PHYSICS

A. Measurements of h_c mass, width and branching fractions

The charmonium mesons are important because of their simplicity and their accessibility by a variety of theoretical approaches, including effective field theories and lattice QCD [22]. Because of their large mass, the charmed quarks bound in the charmonium meson states have relatively low velocities, $v^2 \sim 0.3$, and non-relativistic potential models can be used with relativistic effects treated as small perturbations. With the discovery of the η'_c by Belle in 2002 [23] and the h_c by CLEO in 2005 [24], all of the charmonium states below the $M = 2m_D$ open-charm threshold have been identified (see Fig. 6). An experimental task now is the provision of precision measurements that can challenge the various theories that address this system.

The singlet P -wave h_c meson is notoriously difficult to study. In fact, despite considerable experimental efforts, it evaded detection for some thirty years until it was finally seen by CLEO in 2005 in the isospin-violating $\psi' \rightarrow \pi^0 h_c$ transition (indicated by a magenta arrow in Fig. 6) [24]. To date, it has only been seen by two groups, CLEO and BESIII [25] and only via the strongly suppressed $\psi' \rightarrow \pi^0 h_c$ process.

In lowest-order perturbation theory, the h_c mass is equal to the spin-weighted-average of the triplet P -wave $\chi_{c0,1,2}$ states: $\langle m_{\chi_{cJ}} \rangle = (m_{\chi_{c0}} + 3m_{\chi_{c1}} + 5m_{\chi_{c2}})/9 = 3525.30 \pm 0.04$ MeV. Theoretical predictions for the branching

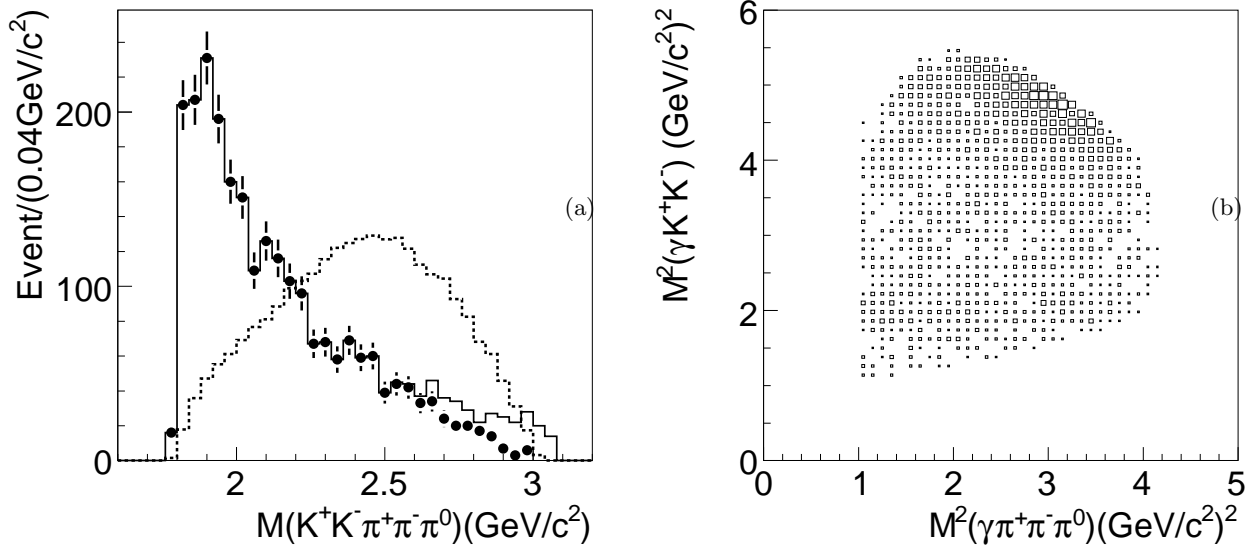


FIG. 5: (a) The invariant-mass distribution of $K^+K^-\pi^+\pi^-\pi^0$; the dashed line is the mass distribution of the phase space MC sample; the solid histogram shows the mass distribution without the requirement of $M(\gamma\pi^+\pi^-\pi^0) > 1.0 \text{ GeV}/c^2$. (b) Dalitz plot of $M^2(\gamma\pi^+\pi^-\pi^0)$ versus $M^2(\gamma K^+K^-)$.

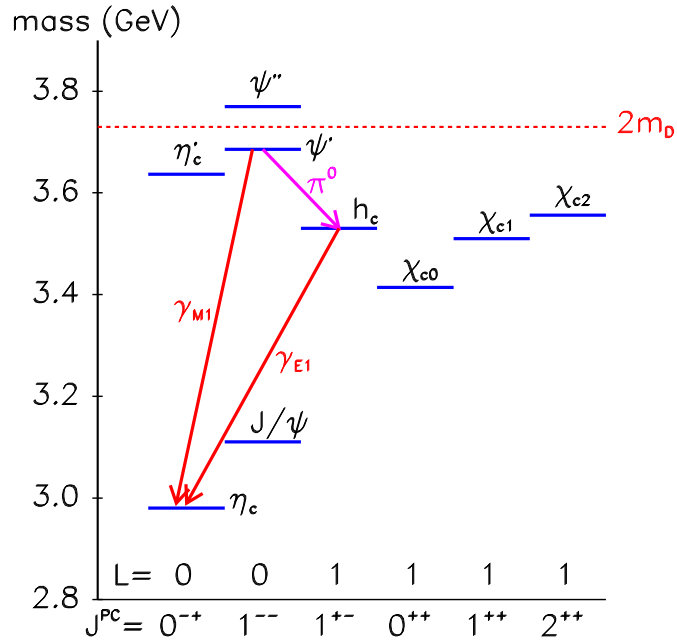


FIG. 6: The spectrum of the low-lying charmonium mesons. The red dashed line indicates the $M = 2m_D$ open-charmed threshold. States with mass above this value can decay to final states containing D and \bar{D} mesons and are typically broad; states below this threshold are relatively narrow. The magenta and red arrows indicate transitions used for the η_c and h_c measurements reported here.

fraction for $\psi' \rightarrow \pi^0 h_c$ are in the range $(0.4 \sim 1.3) \times 10^{-3}$, the E1 radiative transition $h_c \rightarrow \gamma \eta_c$ is expected to be the dominant decay mode with a branching fraction somewhere between $40 \sim 90\%$, and the h_c total width is expected to be less than 1 MeV [26].

Three detection & analysis methods have been used to study h_c production and decay, all of them use the processes indicated by arrows in Fig. 6:

inclusive In the “inclusive” mode, only the π^0 is detected and the h_c shows up as a peak in the mass recoiling against the detected π^0 , which is inferred from conservation of energy and momentum. The inclusive mode signal yield is proportional the $Bf(\psi' \rightarrow \pi^0 h_c)$. This mode has the highest background.

E1-tagged In the “E1-tagged” mode the π^0 and the E1 transition γ from the $h_c \rightarrow \gamma \eta_c$, with energy in the range $465 - 535$ MeV, are detected. The E1-tagged signal yield is proportional to the branching fraction product $Bf(\psi' \rightarrow \gamma h_c) \times Bf(h_c \rightarrow \gamma \eta_c)$. The background for this mode is relatively smaller than that for the inclusive mode.

exclusive In the “exclusive” mode, the π^0 , E1- γ and all of the decay products of the η_c are detected. Here all final-state particles are detected and energy-momentum conserving kinematic fits can be used to improve the resolution. The backgrounds are small and the yield is proportional to a triple product of branching fractions, including that for the η_c decay channel that is detected.

The CLEO observation used both the E1-tagged and exclusive modes. BESII has reported results from the inclusive and E1-tagged modes; an exhaustive study of exclusive channels is in progress.

The BESIII π^0 recoil mass distributions for the E1-tagged and inclusive modes are shown in Fig. 7. The E1-tagged sample (top) has the most distinct signal and this is used to determine the mass and width of the h_c . The solid curve in the figure is the result of a fit using a BW function convolved with a MC-determined resolution function to represent the signal, and a background shape that is determined from events with no photon in the E1 signal region, but with a photon in the E1-tag sidebands. From the fit, the mass and width are determined to be

$$m_{h_c} = 3525.40 \pm 0.22 \text{ MeV} \quad (2)$$

$$\Gamma_{h_c} = 0.73 \pm 0.53 \text{ MeV}; \quad (3)$$

the 90% CL upper limit on the width is $\Gamma_{h_c} < 1.44$ MeV. With this mass value, the P -wave hyperfine splitting is $\langle m_{\chi_{cJ}} \rangle - m_{h_c} = -0.10 \pm 0.22$ MeV, consistent with zero. From the signal yield, the product branching fraction $Bf(\psi' \rightarrow \pi^0 h_c) \times Bf(h_c \rightarrow \gamma \eta_c) = (4.48 \pm 0.64) \times 10^{-4}$ is determined.

The inclusive π^0 recoil mass distribution is shown in the lower part of Fig. 7. Here the solid curve is the result of a fit where the mass and width of the signal function are fixed at the E1-tagged results and the background is parameterized by a fourth-order Chebyshev polynomial with all parameters allowed to float. The signal yield and the product branching fraction results from the E1-tagged mode are used to make the first determination of the individual branching fractions:

$$Bf(\psi' \rightarrow \pi^0 h_c) = (8.4 \pm 1.6) \times 10^{-4} \quad (4)$$

$$Bf(h_c \rightarrow \gamma \eta_c) = (54.3 \pm 8.5)\%, \quad (5)$$

which are within the range of theoretical expectations.

B. Measurement of the η_c mass and width

The η_c is the ground state of the charmonium system. The mass difference between the J/ψ and the η_c is due to hyperfine spin-spin interactions and is, therefore, a quantity of fundamental interest. However, while the mass of the J/ψ is known to very high precision –better than 4 PPM– the η_c mass remains poorly measured, the 2010 PDG world average (WA) value is $m_{\eta_c}^{2010} = 2980.3 \pm 1.2$ MeV, and the measurements that go into this average have poor

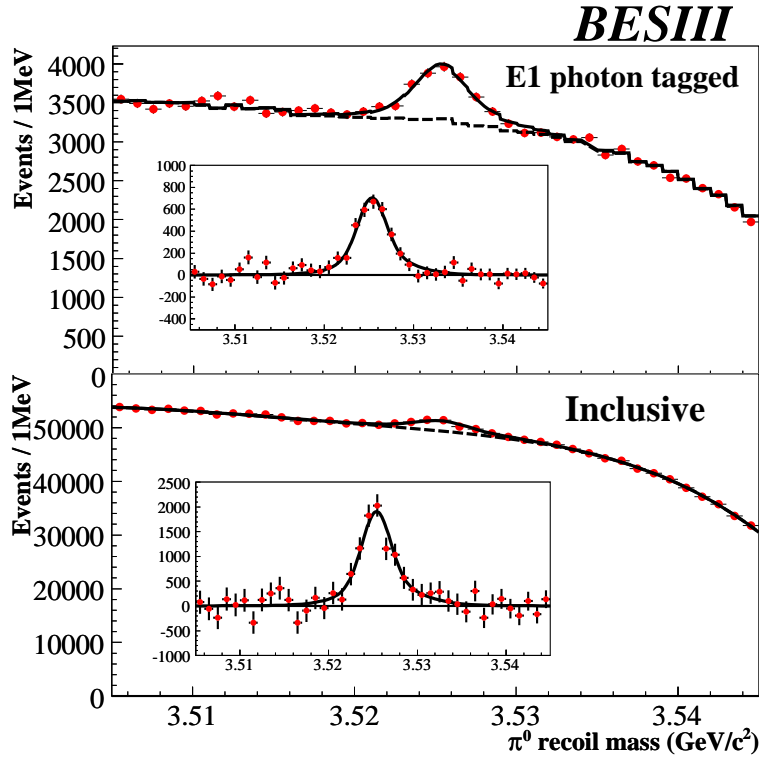


FIG. 7: The π^0 recoil mass for E1-tagged (top) and inclusive (bottom) $\psi' \rightarrow \pi^0 X$ decays. The insets show the signal yields with the fitted backgrounds subtracted.

internal consistency: the CL of the fit to a single mass is only 0.0018. The J/ψ - η_c hyperfine mass splitting derived from this WA is $\delta_{hfs} = 116.6 \pm 1.2$ MeV, a value that has always been above theoretical predictions [27]. The η_c width is also very poorly known; the 2010 PDG WA for this, $\Gamma_{\eta_c}^{2010} = 28.6 \pm 2.2$ MeV, has a confidence level of only 0.0001.

Measurements of the η_c mass and width roughly fall into two categories, depending on how the η_c mesons used in the measurement are produced. Experiments using η_c mesons produced via J/ψ radiative transitions tend to find a low mass (~ 2978 MeV) and narrow width (~ 10 MeV), while measurements using η_c mesons produced via two-photon collisions or B -meson decays find higher mass and width values. A primary early goal of the BESIII experiment has been to try to clear up this situation.

A recently reported BESIII mass and width measurement [28] uses samples of η_c mesons produced via the M1 radiative transition $\psi' \rightarrow \gamma\eta_c$ (indicated by a red arrow in in Fig. 6) that decay to one of six fully reconstructed final states (the inclusion of charge conjugate states is implied): $\eta_c \rightarrow X_i$, where $X_i = K_S K^+ \pi^-$, $K^+ K^- \pi^0$, $\eta \pi^+ \pi^-$, $K_S K^+ \pi^+ \pi^- \pi^-$, $K^+ K^- \pi^+ \pi^- \pi^0$, and $3(\pi^+ \pi^-)$, where $K_S \rightarrow \pi^+ \pi^-$ and $\pi^0 (\eta) \rightarrow \gamma\gamma$. Distinct η_c signals are seen in each of the six channels, two typical mass spectra are shown in Fig. 8.

In all six channels, the η_c signal has a distinctively asymmetric shape with a long tail at low masses and a rapid drop on the high mass side. This is suggestive of possible interference with a coherent non-resonant background. The solid blue curves in Fig. 6 show the results of a fit that uses a Breit Wigner (BW) amplitude to represent the η_c that is weighted by a factor of E_γ^7 that accounts for the M1 transition matrix element (E_γ^3) and the wave-function mismatch between the radially excited ψ' and the ground-state η_c (E_γ^4); the fit also allows for interference with background from nonresonant $\psi' \rightarrow \gamma X_i$ decays. Since fits to individual channels give consistent results for the mass, width and the same value for the interference phase, a global fit to all six channels at once with a single mass, width

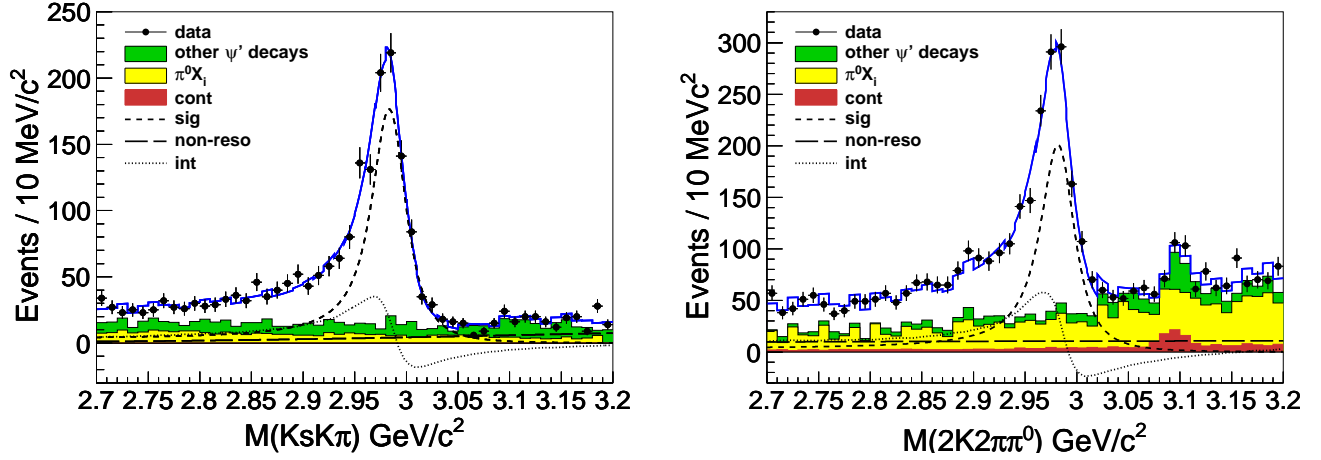


FIG. 8: **Left:** The $K_S K^+ \pi^-$ mass spectrum from $\psi' \rightarrow \gamma K_S K^+ \pi^-$ decays. **Right:** The corresponding plot for the $K^+ K^- \pi^+ \pi^- \pi^0$ channel. The main background in most channels, indicated as yellow histograms, are from $\psi' \rightarrow \pi^0 X_i$, where X_i is the same final state as the η_c decay mode that is under study, and the $\pi^0 \rightarrow \gamma\gamma$ decay is asymmetric where one γ has very low energy and is not detected. This background is incoherent and does not interfere with the η_c signal.

and phase is used to determine the final results:

$$m_{\eta_c} = 2984.3 \pm 0.8 \text{ MeV} \quad (6)$$

$$\Gamma_{\eta_c} = 32.0 \pm 1.6 \text{ MeV}. \quad (7)$$

The value of the phase ϕ depends upon whether the constructive or destructive interference solution is used: $\phi_{cons} = 2.40 \pm 0.11$ or $\phi_{des} = 4.19 \pm 0.09$. (The mass and width values for the two cases are identical.) The reason that the interference phase is the same for all six channels is not understood.

The new BESIII mass and width values agree well with the earlier higher values found in two-photon and B -meson decay measurements. The probable reasons for the low values found by earlier measurements using η_c mesons produced via radiative charmonium decays are the effects of the wave-function mismatch [29] and interference with the non-resonant background that were not considered. Using only the new BESIII η_c mass value, the J/ψ - η_c hyperfine mass splitting becomes smaller: $\delta_{hf_s} = 112.6 \pm 0.8 \text{ MeV}$, and in better agreement with theory.

C. First observation of the M1 transition $\psi' \rightarrow \gamma\eta_c(2S)$

The $\eta_c(2S)$ was first observed by the Belle collaboration in the process $B^\pm \rightarrow K^\pm \eta_c(2S)$, $\eta_c(2S) \rightarrow K_S^0 K^\pm \pi^\mp$ [30]. It was confirmed in the two-photon production of $K_S^0 K^\pm \pi^\mp$ [31, 32], and in the double-charmonium production process $e^+e^- \rightarrow J/\psi c\bar{c}$ [33, 34]. The production of the $\eta_c(2S)$ through a radiative transition from the ψ' requires a charmed-quark spin-flip and, thus, proceeds via a magnetic dipole (M1) transition.

BESIII has reported the first observation of $\psi' \rightarrow \gamma\eta_c(2S)$, with $\eta_c(2S) \rightarrow K_S^0 K^\pm \pi^\mp$ and $K^+ K^- \pi^0$ using 106 M ψ' events [35]. The mass spectra for the $K_S^0 K^\pm \pi^\mp$ and $K^+ K^- \pi^0$ channels and a simultaneous fit to extract the yield, mass and width of $\eta_c(2S)$ are shown in Fig. 9.

Analyses of the processes $\psi' \rightarrow \gamma\eta_c(2S)$ with $\eta_c(2S) \rightarrow K_S^0 K^\pm \pi^\mp$ and $K^+ K^- \pi^0$ gave an $\eta_c(2S)$ signal with a statistical significance of greater than 10 standard deviations under a wide range of assumptions about the signal and background properties. The data are used to obtain measurements of the $\eta_c(2S)$ mass ($M(\eta_c(2S)) = 3637.6 \pm 2.9_{\text{stat}} \pm 1.6_{\text{sys}} \text{ MeV}/c^2$), width ($\Gamma(\eta_c(2S)) = 16.9 \pm 6.4_{\text{stat}} \pm 4.8_{\text{sys}} \text{ MeV}$), and the product branching fraction ($\mathcal{B}(\psi' \rightarrow \gamma\eta_c(2S)) \times \mathcal{B}(\eta_c(2S) \rightarrow K\bar{K}\pi) = (1.30 \pm 0.20_{\text{stat}} \pm 0.30_{\text{sys}}) \times 10^{-5}$). Combining our result with a BaBar measurement of $\mathcal{B}(\eta_c(2S) \rightarrow K\bar{K}\pi)$, we find the branching fraction of the M1 transition to be $\mathcal{B}(\psi' \rightarrow \gamma\eta_c(2S)) = (6.8 \pm 1.1_{\text{stat}} \pm 4.5_{\text{sys}}) \times 10^{-4}$.

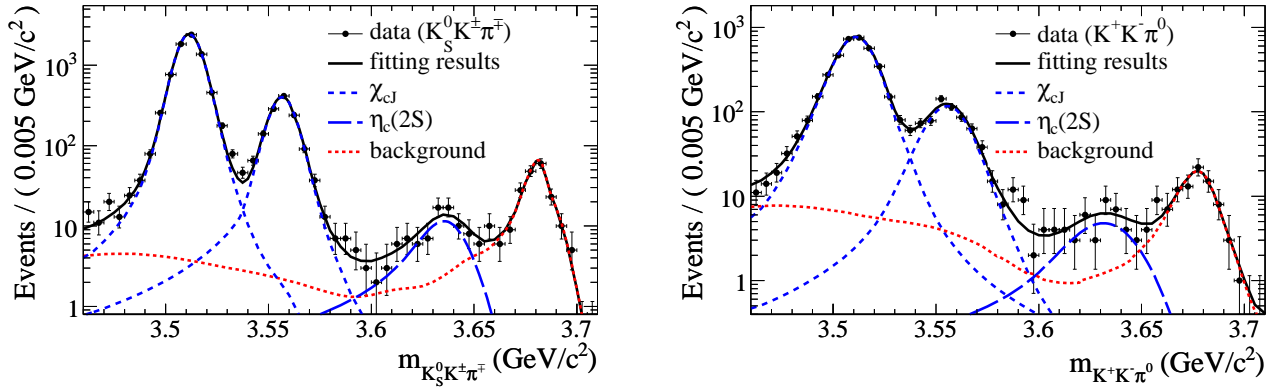


FIG. 9: The invariant-mass spectrum for $K_S^0 K^\pm \pi^\mp$ (left panel), $K^+ K^- \pi^0$ (right panel), and the simultaneous likelihood fit to the three resonances and combined background sources as described in the text.

D. Evidence for $\psi' \rightarrow \gamma\gamma J/\psi$

Two-photon spectroscopy has been a very powerful tool for the study of the excitation spectra of a variety of systems with a wide range of sizes, such as molecules, atomic hydrogen and positronium [36]. Studying the analogous process in quarkonium states is a natural extension of this work, in order to gain insight into non-perturbative QCD phenomena. But so far, two-photon transitions in quarkonia have eluded experimental observation [37–39]. For example, in a study of $\psi' \rightarrow \gamma\chi_{cJ}(J = 0, 1, 2)$ reported by CLEO-c [39], the upper limit for $\mathcal{B}(\psi' \rightarrow \gamma\gamma J/\psi)$ was estimated to be 1×10^{-3} .

BESIII has reported the first evidence for the two-photon transition $\psi' \rightarrow \gamma\gamma J/\psi$, studies of the orientation of the ψ' decay plane and the J/ψ polarization in the decay, as well as the branching fractions of double $E1$ transitions $\psi' \rightarrow \gamma(\gamma J/\psi)_{\chi_{cJ}}$ through χ_{cJ} intermediate states. The yield of the signal process $\psi' \rightarrow \gamma\gamma J/\psi$, together with those of the cascade $E1$ transition processes, is estimated by a global fit to the spectrum of $RM_{\gamma_{sm}}$. The fit results are shown in Fig. 10. The $\psi' \rightarrow \gamma\gamma J/\psi$ transition is observed with a statistical significance of 6.6σ . When the systematic uncertainties are taken into account with the assumption of Gaussian distributions, the significance is evaluated to be 3.8σ . A cross-check on the procedures is performed with the $RM_{\gamma\gamma}$ spectrum for the events in the region $3.44 \text{ GeV}/c^2 < RM_{\gamma_{sm}} < 3.48 \text{ GeV}/c^2$ without restriction on $RM_{\gamma\gamma}$, as shown in Fig. 10(e) and (f). An excess of data above known backgrounds can be seen around the J/ψ nominal mass, which is expected from the sought-after two-photon process. With the inclusion of the estimated yields of the signal process, the excess is well understood. The branching fraction of $\psi' \rightarrow \gamma\gamma J/\psi$ is determined to be $(3.3 \pm 0.6(\text{stat})_{-1.1}^{+0.8}(\text{syst})) \times 10^{-4}$ (preliminary) using $J/\psi \rightarrow e^+e^-$ and $J/\psi \rightarrow \mu^+\mu^-$ decays [40].

IV. CHARMED MESON PHYSICS

The primary goal of the BESIII program is precision studies of weak decay processes of D and D_s mesons. The initial phase of this program was a long data-taking run that accumulated 2.9 fb^{-1} at the peak of the $\psi(3770)$ charmonium meson. This is a resonance in the $e^+e^- \rightarrow D\bar{D}$ channel with a peak cross section of about 6 nb at a c.m. energy that is about 40 MeV above the $E_{c.m.} = 2m_D$ open-charm mass threshold. The $\psi(3770)$ is included in the sketch of the charmonium spectrum shown in Fig. 6.

The 2.9 fb^{-1} data sample that has already been collected contains almost 20M $D\bar{D}$ meson pairs and is about three times the world's previous largest $\psi(3770)$ event sample collected by CLEO-c and is currently being used for numerous analyses aimed at searches for rare decays and new physics, and improving on the precision of previous

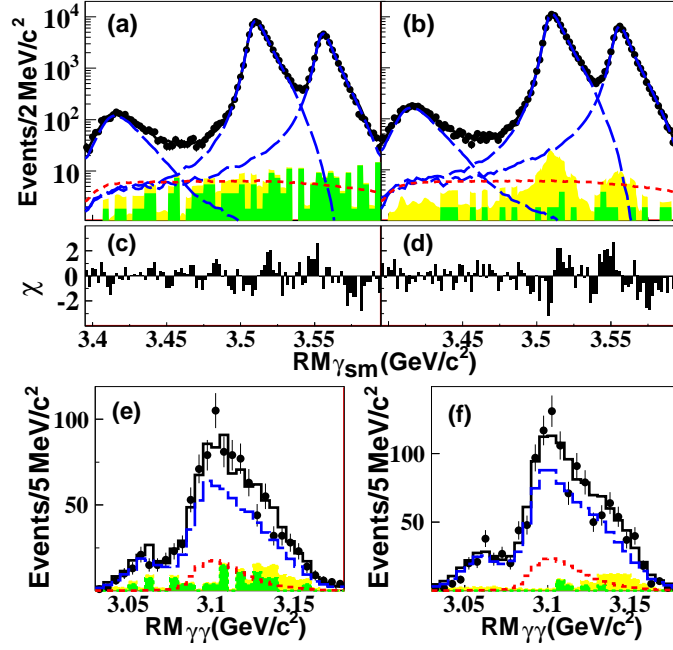


FIG. 10: (color online) Plot a(b): unbinned maximum likelihood fit to the distribution of $RM_{\gamma sm}$ in data for $\gamma\gamma e^+e^-$ ($\gamma\gamma\mu^+\mu^-$) mode. Thick lines are the sum of the fitting models and long-dashed lines the χ_{cJ} shapes. Short-dashed lines represent the two-photon signal processes. Shaded histograms are ψ' -decay backgrounds (yellow) and non- ψ' backgrounds (green), with the fixed amplitude and shape taken from MC simulation and continuum data. Plot c(d): the number of standard deviations, χ , of data points from the fitted curves in plot a(b). The rates of the signal process and sequential χ_{cJ} processes are derived from these fits. Plot e(f): distributions of $RM_{\gamma\gamma}$ in data, the signal process and known backgrounds with kinematic requirement $3.44 \text{ GeV}/c^2 < RM_{\gamma sm} < 3.48 \text{ GeV}/c^2$ and with removal of $RM_{\gamma\gamma}$ window requirement for $\gamma\gamma e^+e^-$ ($\gamma\gamma\mu^+\mu^-$) mode.

measurements. In many of the latter cases, the measurements are of form-factors that are accessible in lattice QCD calculations. As the precision of lattice QCD improves, BESIII will provide more precise measurements that continue to challenge the theory.

A. D tagging technique

Most of $\psi(3770)$ decays are to $D\bar{D}$ meson pairs and nothing else, because there is not enough enough c.m. energy to produce any other accompanying hadrons. As a result, The energy of each D meson is half of the total c.m. energy, which is precisely known. Thus, when a D meson is reconstructed in an event, the recoil system is “tagged” as a \bar{D} , and the constraint on the energy results in reconstructed D -meson mass signals that have excellent resolution ($\sigma = 1.3 \text{ MeV}$ for all charged modes and $\sigma = 1.9 \text{ MeV}$ for modes with one π^0) and signal to noise. As examples, D^- meson signals for nine commonly used tag decay modes are shown in Fig. 11. A maximum likelihood fit to the mass spectrum with a Crystal Ball function plus an Gaussian function for the D^- signal and the ARGUS function to describe background yields the number of the singly tagged D^- events for each of the nine modes. Selecting these candidates for D^- tags within the range marked by arrows in Fig. 11 reduce signal number by about 2% giving a total of $1586056 \pm 2327 D^-$ tags. In these D^- tags, 20103 D^- tags are reconstructed in more than one single D^- tag mode. Subtracting this number of the double counting D^- tags from the $1586056 \pm 2327 D^-$ tags yields $1565953 \pm 2327 D^-$ tags which are used for further analysis of measuring the branching fraction for $D^+ \rightarrow \mu^+\nu_\mu$ decays. Moreover, the $D\bar{D}$ system is in a coherent, P -wave quantum state with $J^{PC} = 1^{--}$. This coherence is unique to D mesons originating from $\psi(3770) \rightarrow D\bar{D}$ decays and permits a number of interesting measurements [41]. For example, if one D meson is tagged in a pure CP decay mode (such as K^+K^- , $\pi^+\pi^-$ or $K_S\pi^0\pi^0$ for $CP = +1$, and $K_S\pi^0$, $K_S\eta$ or $K_S\omega$ for $CP = -1$), the decay of the accompanying D meson to a CP eigenstate with the same

CP eigenvalue would be an unambiguous signal for CP violation.

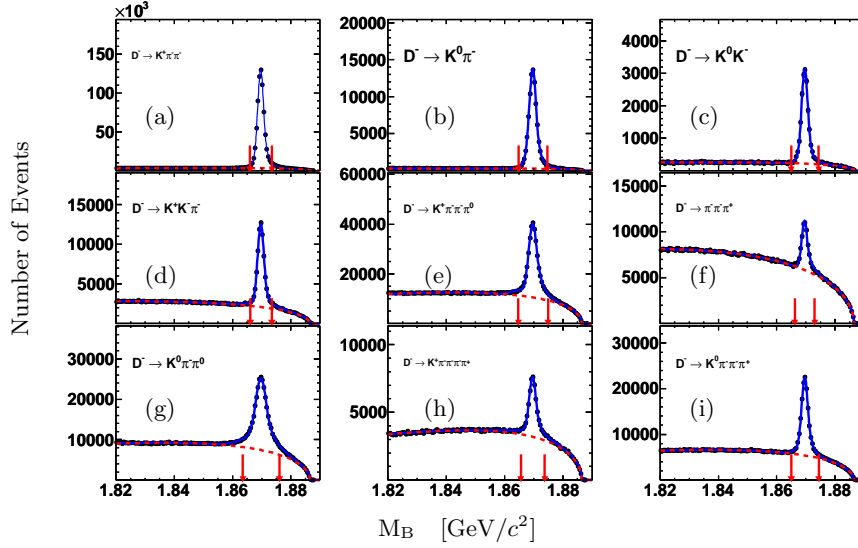


FIG. 11: Distributions of the beam energy constraint masses of the $mKn\pi$ combinations for the 9 single tag modes from the data; where (a), (b), (c), (d), (e), (f), (g), (h), (i) are for the modes of $D^- \rightarrow K^+\pi^-\pi^-$, $D^- \rightarrow K_s^0\pi^-$, $D^- \rightarrow K_s^0K^-$, $D^- \rightarrow K^+K^-\pi^-$, $D^- \rightarrow K^+\pi^-\pi^-\pi^0$, $D^- \rightarrow \pi^+\pi^-\pi^-$, $D^- \rightarrow K_s^0\pi^-\pi^0$, $D^- \rightarrow K^+\pi^-\pi^-\pi^+$, and $D^- \rightarrow K_s^0\pi^-\pi^-\pi^+$, respectively.

B. Leptonic decays of D^+ meson

In the SM (Standard Model) of particle physics, the D^+ meson can decay into $l^+\nu_l$ (where l is e , μ or τ) through a virtual W^+ boson. The decay rate is determined by the wavefunction overlap of the two quarks at the origin, and is parameterized by the D^+ decay constant, f_{D^+} . To the lowest order, as the analogue of the decay width of $\pi^+ \rightarrow l^+\nu_l$, the decay width of $D^+ \rightarrow l^+\nu_l$ is given by

$$\Gamma(D^+ \rightarrow l^+\nu_l) = \frac{G_F^2 f_{D^+}^2}{8\pi} |V_{cd}|^2 m_l^2 m_{D^+} \left(1 - \frac{m_l^2}{m_{D^+}^2}\right)^2, \quad (8)$$

where G_F is the Fermi coupling constant, V_{cd} is the Cabibbo-Kobayashi-Maskawa (CKM) matrix element between the two quarks $c\bar{d}$ [12] in D^+ , m_l is the mass of the lepton, and m_{D^+} is the D^+ mass. By measuring the branching fraction of $D^+ \rightarrow \mu^+\nu_\mu$, the decay constant f_{D^+} can be determined.

Candidate events for the decay $D^+ \rightarrow \mu^+\nu_\mu$ are selected from the surviving charged tracks in the system recoiling against the singly tagged D^- mesons. To select the $D^+ \rightarrow \mu^+\nu_\mu$, it is required that there be a single charged track originating from the interaction region in the system recoiling against the D^- tag and the charged track satisfies $|\cos\theta| < 0.93$ as well as it is identified as a μ^+ . The μ^+ can be well identified with the passage length of a charged particle through the MUC since a charged hadron (pion or kaon) quickly loses its energy due to its strong interactions with the absorber of the MUC and most of the hadrons stop in the absorber before passing a long passage length in the MUC. For the candidate event, no extra good photon which is not used in the reconstruction of the singly tagged D^- meson is allowed to be present in the event, where the “good photon” is the one with deposited energy in the EMC being greater than 300 MeV.

Since there is a missing neutrino in the purely leptonic decay event, the event should be characteristic with missing energy E_{miss} and missing momentum p_{miss} which are carried away by the neutrino. So they infer the existence of

the neutrino by requiring a measured value of the missing mass squared M_{miss}^2 to be around zero. The missing mass squared M_{miss}^2 is defined as

$$M_{\text{miss}}^2 = (E_{\text{beam}} - E_{\mu^+})^2 - (-\vec{p}_{D_{\text{tag}}^-} - \vec{p}_{\mu^+})^2, \quad (9)$$

where E_{μ^+} and \vec{p}_{μ^+} are, respectively, the energy and three-momentum of the μ^+ , and $\vec{p}_{D_{\text{tag}}^-}$ is three-momentum of the candidate for D^- tag.

Figure 12(a) and (b) show the scatter-plots of the momentum of the identified muon satisfying the requirement for selecting $D^+ \rightarrow \mu^+ \nu_\mu$ decay versus M_{miss}^2 , where the blue box in Fig. 12(a) shows the signal region for $D^+ \rightarrow \mu^+ \nu_\mu$ decays. Within the signal region, there are 425 candidate events for $D^+ \rightarrow \mu^+ \nu_\mu$ decay. The two concentrated clusters outside of the signal region are from D^+ non-leptonic decays and some other background events. The events whose peak is around $0.25 \text{ GeV}^2/c^4$ in M_{miss}^2 are mainly from $D^+ \rightarrow K_L^0 \pi^+$ decays, where K_L^0 is missing. Projecting the events for which the identified muon momentum being in the range from 0.8 to 1.1 GeV/c onto the horizontal scale yields the M_{miss}^2 distribution as shown in Fig. 12(c), where the difficultly suppressed backgrounds from $D^+ \rightarrow K_L^0 \pi^+$ decays in CLEO-c measurement [42] are effectively suppressed due to that they use the MUC measurements to identify the muon.

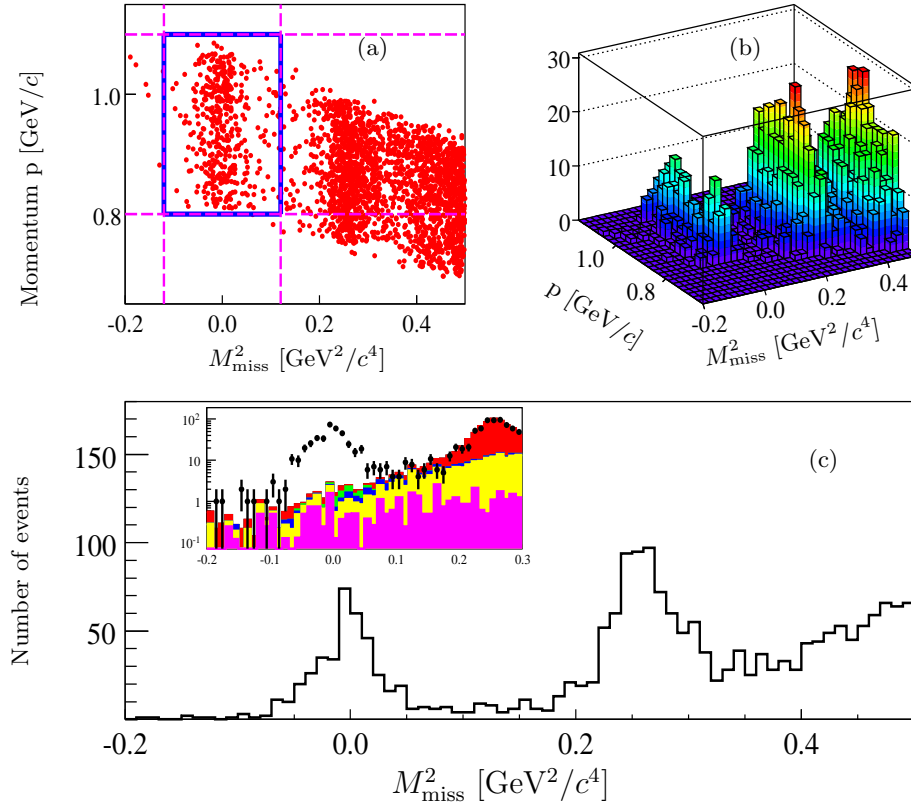


FIG. 12: Distributions of M_{miss}^2 , where (a) and (b) are scatter plots of the identified muon momentum p VS M_{miss}^2 , and (c) is the distribution of M_{miss}^2 . The insert shows the signal region for $D^+ \rightarrow \mu^+ \nu_\mu$ on a log scale, where dots with error bars are for the data, histograms are for the simulated backgrounds from $D^+ \rightarrow K_L^0 \pi^+$ (red), $D^+ \rightarrow \pi^0 \pi^+$ (green), $D^+ \rightarrow \tau^+ \nu_\tau$ (blue) and other decays of D mesons (yellow) as well as from $e^+ e^- \rightarrow \text{non-}D\bar{D}$ decays (pink).

Some non-purely leptonic decay events from the D^+ , D^0 , $\gamma\psi(3686)$, $\gamma J/\psi$, $\psi(3770) \rightarrow \text{non-}D\bar{D}$, $\tau^+ \tau^-$ decays as well as continuum light hadron production may also satisfy the selection criteria and are the background events to the purely leptonic decay events. These background events must be subtracted off. The number of the background events can be estimated by analyzing different kinds of Monte Carlo simulation events. Detailed Monte Carlo studies

show that there are $47.7 \pm 2.3 \pm 1.3$ background events in 425 candidates for $D^+ \rightarrow \mu^+ \nu_\mu$ decays, where the first error is due to Monte Carlo statistic and second systematic arising from uncertainties in the branching fractions or production cross sections.

After subtracting the number of background events, $377.3 \pm 20.6 \pm 2.6$ signal events for $D^+ \rightarrow \mu^+ \nu_\mu$ decay are retained, where the first error is statistical and the second systematic arising from the uncertainty of the background estimation.

The overall efficiency for observing the decay $D^+ \rightarrow \mu^+ \nu_\mu$ is obtained by analyzing full Monte Carlo simulation events of $D^+ \rightarrow \mu^+ \nu_\mu$ VS D^- tags and combining with μ^+ reconstruction efficiency in the MUC. The μ^+ reconstruction efficiency in the MUC is measured with muon samples selected from the same data taken at 3.773 GeV. The overall efficiency is 0.6382 ± 0.0015 .

With 1565953 singly tagged D^- mesons, $377.3 \pm 20.6 \pm 2.6$ $D^+ \rightarrow \mu^+ \nu_\mu$ decay events observed and the efficiency 0.6382 ± 0.0015 , the BES-III collaboration obtain the branching fraction

$$B(D^+ \rightarrow \mu^+ \nu_\mu) = (3.74 \pm 0.21 \pm 0.06) \times 10^{-4} \quad (\text{BESIII Preliminary}),$$

where the first error is statistical and the second systematic. This measured branching fraction is consistent within error with world average of $B(D^+ \rightarrow \mu^+ \nu_\mu) = (3.82 \pm 0.33) \times 10^{-4}$ [12], but with more precision.

The decay constant f_{D^+} can be obtained by inserting the measured branching fraction, the mass of the muon, the mass of the D^+ meson, the CKM matrix element $|V_{cd}| = 0.2252 \pm 0.0007$ from the CKMFitter [12] G_F and the lifetime of the D^+ meson [12] into Eq.(8), which yields

$$f_{D^+} = (203.91 \pm 5.72 \pm 1.97) \text{ MeV} \quad (\text{BESIII Preliminary}),$$

where the first errors are statistical and the second systematic arising mainly from the uncertainties in the measured branching fraction (1.7%), the CKM matrix element $|V_{cd}|$ (0.3%), and the lifetime of the D^+ meson (0.7%) [12]. The total systematic error is 1.0%.

C. Semi-leptonic decays of D^0 meson

Semileptonic decays are an excellent environment for precision measurements of the Cabibbo-Kobayashi-Maskawa (CKM) matrix elements. However, Extract of the CKM weak parameters require knowledge of strong interaction effects. These can be parametrized by form factors. Techniques such as lattice quantum chromodynamics offer increasingly precise calculations of these form factors, but as the uncertainties in the predictions shrink, experimental validation of the results becomes increasingly important.

The D^0 mesons are produced from decays $\psi(3770) \rightarrow D^0 \bar{D}^0$. The tagged- D^0 is reconstructed from four hadronic modes. The amount of signal events is determined by fitting the distribution of $U_{miss} = E_{miss} - |\vec{p}_{miss}|$. Based on data sample of 0.92 fb^{-1} , preliminary results on the branching fractions are measured as: $\mathcal{B}(\bar{D}^0 \rightarrow K^+ e^- \nu) = (3.542 \pm 0.030 \pm 0.067) \times 10^{-2}$ and $\mathcal{B}(\bar{D}^0 \rightarrow \pi^+ e^- \nu) = (0.288 \pm 0.008 \pm 0.005) \times 10^{-2}$. Note that results are based on approximately one third of the statistics and systematic errors are preliminary. The analysis with the full 2.9 fb^{-1} data and the form factor measurement are ongoing.

D. $D^0 \rightarrow \gamma\gamma$

In the Standard Model flavor-changing neutral currents are forbidden at tree level [43]. These decays are allowed at higher order. To date, measurements of radiative decays of charm mesons are consistent with results of theoretical calculations that include both short-distance and long-distance contributions and predict decay rates several orders of magnitude below the sensitivity of current experiments. While these rates are small, it has been postulated that new physics processes can lead to significant enhancements [44].

The D^0 mesons are produced from $\psi(3770) \rightarrow D^0 \bar{D}^0$. The signal yields for $D^0 \rightarrow \gamma\gamma$ is obtained by fitting the distribution $\Delta E = E_{\gamma\gamma} - E_{beam}$. No signal is observed. The upper limit of branching fraction is determined to be $\mathcal{B}(D^0 \gamma\gamma) < 4.6 \times 10^{-6}$ (preliminary) at 90% confidence level. This upper limit is tighter than that in PDG [12] but not as stringent as measured by BaBar Collaboration (2.4×10^{-6}) [45].

V. OTHER ACTIVITIES

A. τ mass measurement

As fundamental parameters of the standard model, masses of quarks and leptons cannot be determined by the theory and must be measured. A precise measurement of the mass of the τ lepton is important for testing lepton universality and for calculating branching fractions that depend on the τ mass. The τ mass measurement benefits from a high-precision beam-energy monitor based on the detection of Compton scattering of back-scattered photons from a high powered single-mode infrared laser. This system has been commissioned and routinely measures the beam energy with a precision of $\delta_{E_{beam}}/E_{beam} \simeq 10^{-5}$ [46]. A optimized energy scan near the τ pair production threshold has been performed. About 24 pb^{-1} of data, distributed over 4 scan points, have been collected. This work is based on the combined data from the $ee, e\mu, eh, \mu\mu, \mu h, hh, e\rho, \mu\rho$ and $\pi\rho$ final states, where h denotes a charged π or K . The mass of the τ lepton is measured from a maximum likelihood fit to the τ pair production cross section data which yields the value of m_τ with a precision $< 0.3 \text{ MeV}$. With 100 pb^{-1} data planned later this year, the precision will eventually reach to $< 0.1 \text{ MeV}$.

B. Additional J/ψ and ψ' data samples.

Most of the results reported above are based on 106M event ψ' and 225M event J/ψ data samples. Earlier this year BESIII collected another $\sim 0.4\text{B}$ ψ' events and $\sim 1.0\text{B}$ J/ψ events. These samples will be used, among other things, for detailed PWA of the many unassigned resonance peaks that have been seen, studies of baryon spectroscopy, and high-statistics measurements of isospin-violating processes that are proving to be valuable probes of the structure of near-threshold resonances. In addition, with the huge J/ψ data sample, the expected SM level for weak decays of the J/ψ to final states containing a single D or D_s meson can be accessed and searches for non-SM weak decays and lepton-flavor-violating decays, such as $J/\psi \rightarrow e^+ \mu^-$, will have interesting sensitivity.

C. R measurement and QCD studies

Before shutdown for summer maintenance this year, BESIII also collected data at 4 low energies: 2.23, 2.4, 2.8 and 3.4 GeV. At each energy point, the number of inclusive hadronic events is more than $10k$, which will reduce the statistics uncertainty for R measurement down to 1% level, and thus make it possible for a $\sim 3\%$ precision measurement.

Other QCD studies, like fragmentation function, baryon form factors, multihadron production, are also expected with the data samples.

VI. CONCLUDING REMARKS AND FUTURE PROSPECT

The BESIII experiment at the Institute of High Energy Physics in Beijing, China is up and running and producing interesting results on a variety of topics. The BEPCII collider is performing near design levels and the BESIII detector performance is excellent. We expect to produce many interesting new results in the coming decade.

BESIII plans to redo the total cross section measurements for $e^+e^- \rightarrow \text{hadrons}$ with higher precision over the entire accessible c.m. energy range, measure π^0 and η form factors in two-photon collisions, remeasure the τ mass with much improved accuracy, and do studies of the recently discovered XYZ mesons.

Cross section measurement scans will cover c.m. energies from near the nucleon-antinucleon threshold up to the $\Lambda_c^+\Lambda_c^-$ threshold. The data near the nucleon-antinucleon threshold will be used to measure neutron form factors [47].

Data taken in a dedicated run at $E_{c.m.} \simeq 4260$ MeV will be used to study $Y(4260)$ decays. Sensitive searches for possible new, exotic mesons that decay to π^+J/ψ and π^+h_c , analogous to the $Z_1(10610)^+$ and $Z_2(10650)^+$ mesons seen by Belle in the $b\bar{b}$ bottomonium meson system [48], will be performed for $\pi^+\pi^-J/\psi$ and $\pi^+\pi^-h_c$ final states.

Ultimately, over the next a few years, BESIII intends to collect a total of $\sim 10 \text{ fb}^{-1}$ at the $\psi(3770)$ for D meson measurements and a comparable sample at higher energy, e.g. 4.17 GeV, for D_s meson studies.

VII. ACKNOWLEDGEMENTS

I appreciate the hard work by the local committee for organizing the meeting, especially by Prof. Qun Wang and Prof. Zhengguo Zhao. I thank my BESIII colleagues for allowing me to represent them and for generating the results discussed herein. Liaoyuan Dong and Changzheng Yuan provided materials for preparing my presentation, and I also benefited from informative conversations with Haibo Li, Gang Rong, and suggestions from Xiaorui Lu. The BESIII collaboration thanks the staff of BEPCII and the computing center for their hard efforts.

-
- [1] J.Z. Bai *et al.* (BES Collaboration), Phys. Rev. Lett. **69**, 3021 (1992).
 - [2] J.Z. Bai *et al.* (BES Collaboration), Phys. Rev. Lett. **84**, 594 (2000).
 - [3] J.Z. Bai *et al.* (BESII Collaboration), Phys. Rev. Lett. **88**, 101802 (2002).
 - [4] H. Burkhardt and B. Pietrzyk, Phys. Lett. **B513**, 46 (2001).
 - [5] M. Ablikim *et al.* (BESII Collaboration), Phys. Lett. **B598**, 149 (2004).
 - [6] M. Ablikim *et al.* (BESII Collaboration), Phys. Lett. **B633**, 681 (2006).
 - [7] J.Z. Bai *et al.* (BESII Collaboration), Phys. Rev. Lett. **91**, 022001 (2003).
 - [8] M. Ablikim *et al.* (BESIII Collaboration), Phys. Rev. Lett. **108**, 112003 (2012); see also M. Ablikim *et al.* (BESIII Collaboration), Chin. Phys. C **34**, 421 (2010).
 - [9] E. Klempt, F. Bradamante, A. Martin and J.M. Richard, Phys. Rep. **368**, 119 (2002).
 - [10] M. Ablikim *et al.* (BESIII Collaboration), Phys.Rev.Lett. **108**, 182001 (2012).
 - [11] J.J. Wu, X.-H. Liu, Q. Zhao and B.S. Zou, Phys. Rev. Lett. **108**, 081803 (2012).
 - [12] K. Nakamura, *et al.* (Particle Data Group), Jour. Phys. G **37**, 075021 (2010).
 - [13] M. Ablikim *et al.* (BESIII Collaboration), Phys.Lett. B710, 594 (2012).
 - [14] M. Ablikim *et al.* [BES Collaboration], Phys. Rev. Lett. **96**, 162002 (2006).
 - [15] Köpke L, Vermes N. J/ψ Decays. CERN-EP/88-93, Physics Reports 174 (1989) 67-227: CERN, CH-1211 Geneva 23, Switzerland.
 - [16] B. A. Li, Phys. Rev. D **74**, 054017 (2006).
 - [17] K. T. Chao, hep-ph/0602190.
 - [18] P. Bicudo *et al.*, Eur. Phys. J. C **52**, 363–374 (2007)
 - [19] Q. Zhao *et al.*, Phys. Rev. D **74**, 114025 (2006).
 - [20] D. V. Bugg, hep-ph/0603018.
 - [21] C. Liu *et al.* [Belle Collaboration], Phys. Rev. D **79**, 0701102(R)(2009).
 - [22] For a recent review see N. Brambilla *et al.*, Eur. Phys. J. C **71**, 1534 (2011).
 - [23] S.-K. Choi *et al.* (Belle Collaboration), Phys. Rev. Lett. **89**, 102001 (2002).
 - [24] J. Rosner *et al.* (CLEO Collaboration), Phys. Rev. Lett. **95**, 102003 (2005).
 - [25] M. Ablikim *et al.* (BESIII Collaboration), Phys. Rev. Lett. **104**, 132002 (2010).
 - [26] Y.P. Kuang, S.F. Tuan and T.M. Yan Phys. Rev. D **37**, 1210 (1988), P. Ko, Phys. Rev. D **52**, 1710 (1995), Y.P. Kuang, Phys. Rev. D **65**, 094024 (2002), and S. Godfrey and J. Rosner, Phys. Rev. D **66**, 014012 (2002).

- [27] See, for example, G. Bali *et al.*, PoS LATTICE2010, 134 (2011), arXiv:1011.2195 [hep-lat].
- [28] M. Ablikim *et al.* (BESIII Collaboration), Phys.Rev.Lett. 108, 222002 (2012).
- [29] R. Mitchell *et al.* (CLEO Collaboration), Phys. Rev. Lett. **102**, 011801 (2009).
- [30] S.-K. Choi *et al.* (Belle Collaboration), Phys. Rev. Lett. **89**, 102001 (2002).
- [31] B. Aubert *et al.* (BaBar Collaboration), Phys. Rev. Lett. **92**, 142002 (2004).
- [32] D. M. Asner *et al.* (CLEO Collaboration), Phys. Rev. Lett. **92**, 142001 (2004).
- [33] K. Abe *et al.* (Belle Collaboration), Phys. Rev. Lett. **89**, 142001 (2002).
- [34] B. Aubert *et al.* (BaBar Collaboration), Phys. Rev. D **72**, 031101 (2005).
- [35] M. Ablikim *et al.* (BESIII Collaboration), Phys. Rev. Lett. **109**, 042003 (2012).
- [36] K. Pachucki *et al.*, J. Phys. B **29**, 177 (1996); A. Quattronani and F. Bassani, Phys. Rev. Lett. **50**, 1258 (1983).
- [37] J. Z. Bai *et al.* [BES Collaboration], Phys. Rev. D **70**, 012006 (2004); M. Ablikim *et al.* [BES Collaboration], Phys. Rev. D **71**, 092002 (2005).
- [38] N. E. Adam *et al.* [CLEO Collaboration], Phys. Rev. Lett. **94**, 232002 (2005).
- [39] H. Mendez *et al.* [CLEO Collaboration], Phys. Rev. D **78**, 011102 (2008).
- [40] M. Ablikim *et al.* (BESIII Collaboration), arXiv:1204.0246.
- [41] See, for example, D.M. Asner and W.M. Sun, Phys. Rev. D **73**, 034024 (2006).
- [42] B.I. Eisenstein *et al.* (CLEO Collaboration), Phys. Rev. D **78**, 052003 (2008).
- [43] S. L. Glashow, J. Iliopoulos, and L. Maiani, Phys. Rev. D **2**, 1285 (Oct 1970).
- [44] S. Prelovsek and D. Wyler, Phys. Lett. B **500**, 304 (2001), hep-ph/0012116.
- [45] J. P. Lees *et al.* (BarBar Collaboration), Phys. Rev. D **85**, 091107(R) (2012).
- [46] E.V. Abakumova *et al.*, Nucl. Instrum. Meth. **A659**, 21 (2011).
- [47] R. Baldini, S. Pacetti and A. Zallo, Nucl. Phys. Proc. Suppl. **219-220**, 32 (2011).
- [48] A. Bondar *et al.* (Belle Collaboration), Phys.Rev.Lett. 108, 122001 (2012).